SSRG International Journal of Electronics and Communication Engineering
ISSN: 2348-8549/ https://doi.org/10.14445/23488549/IJECE-V12I1P115

Volume 12 Issue 1, 193-201, January 2025

Original Article

Parametric Analysis of a New Defect Ground Structure-Based Five-Pole Hairpin Bandpass Filter for 5G Applications

Shereen Abdalkadum Shandal

Department of Computer Techniques Engineering, Middle Technical University, Baghdad, Iraq.

Corresponding Author : shereen@mtu.edu.iq

Received: 19 November 2024 Revised: 25 December 2024 Accepted: 12 January 2025 Published: 30 January 2025

Abstract - *In this research, a five-pole hairpin structure is designed, analyzed, simulated, and fabricated on the top layer of the substrate using different Defect Ground Structure (DGS) techniques utilizing the upper and lower layers of the suggested filter. Demand for such filters has grown due to recent trends in tiny size and enhanced filter performance, notably in scattering parameters and broader bandwidth. The DGS at the top layer includes a series of consecutive grooves etched at the first and fifth resonators. While thin rectangular slots are etched at the bottom layer, this design is considered an enhancement over present works. Consequentially, FR4 substrate with permittivity of 1.6 and 1.55 thickness was used to fabricate this filter. Four important parameters have been optimized through parametric optimization; these are the 12mm resonator length Lr, the (11.1×0.1) mm^2 area of DGS at the bottom layer, the 5.5mm feed point position t, and the 0.1mm and 0.2mm spacing between two adjacent hairpin resonators, which have different values designated as S1 and S2, respectively. The simulation results were obtained using High-Frequency Structure Simulator (HFSS) software. The presented filter works within a bandwidth of (2.15 - 3.88) GHz and a 3GHz center frequency. The obtained insertion and return loss values at the passband region are -1.17dB and -56.19 dB. Another software simulator verifies this simulation result, Computer Simulation Technology (CST). Furthermore, this produced filter demonstrates design validity, with outcomes of measurement closely aligning with anticipated outcomes, making it appropriate for diverse Fifth-Generation (5G) applications.*

Keywords - *Five-pole hairpin, Defect ground structure, Insertion loss, Fractional bandwidth, group delay, Vector Network Analyzer.*

1. Introduction

Many microwave/RF wireless communication applications use bandpass filters to permit a certain frequency range to pass and attenuate outside that range [1–4]. The microstrip technique is widely used to realize bandpass filters because it offers small size, cost-effectiveness, and lightweight, and it is simple to integrate into Printed Circuit Boards (PCBs). It is better than the traditional approach, which uses lumped elements as inductors and capacitors [5–8]. A hairpin bandpass filter consists of a series of hairpin-shaped parallel coupled lines. These lines can be put together in different ways to get the needed filter specifications [9, 10]. A hairpin's advantage is its compact size, making this filter ideal for applications that require limited space. Each hairpin is a resonator, and the coupling between two consecutive resonators determines filter selectivity and bandwidth [11–14]. Defected Ground Structures (DGS) are various patterns printed into the bottom layer of a microstrip line in order to improve the filter's performance by altering its electromagnetic properties [15, 16]. Defected Ground Structures (DGS) can assume various shapes, such as rectangular, circular, U-shaped, H-shaped, and interdigital, and their distribution in the ground layer can be either periodic or aperiodic. The design of an S-band filter in [17] achieved a wide stop band attenuation and size reduction through double equilateral U-shaped DGS. A novel compact bandpass filter with a hairpin shape DGS is designed in [18] using the coupling matric method, which resonates at 2GHz with bandwidth in the passband region (1.9-2.5) GHz and -40dB return loss S11. A novel hairpin-line narrow band microstrip bandpass filter with two square-shaped DGS was designed in [19], which has a center frequency of 2.2GHz used for satellite and radar communications with a frequency range (1.9-2.4) GHz and a return loss value -46.64dB. A dumbbell-shaped DGS is utilized in [20] to design a compact bandpass filter with a coplanar waveguide transmission line that operates at multi-band 3.1GHz, 6.8GHz, and 10.6GHz. It has improved return loss S11 values to less than -20dB. A researcher in [21] designed a hairpin filter with DGS operating at (2.9-3.1)GHz used for S-band radar applications with bandwidth 200MHz and return loss S11 less than -20dB; the DGS is added as a square groove to decrease the size of the filter and harmonic suppression with increased return loss. Two various shapes of DGS are used to design a hairpin bandpass filter presented in [22], which operates at 2.4GHz and has a return loss of -26dB; it has a high selectivity and wide bandwidth within the passband region. A planar filter with three DGS resonators is presented in [23], which is used for ISM band applications at 2.4 GHz; the obtained bandwidth is 280MHz, and the DGS has the advantage of suppressing passband spurious. In [24], an open loop microstrip structure is used as a DGS to design a three-pole hairpin bandpass filter for the Very Small Aperture Terminal (VSAT) system, the observed return loss -13dB with the triple band at 10.2GHz, 12.2GHz, and 14.8GHz. In [25], a rectangular-shaped open loop DGS is utilized to design a bandpass filter with a tunable cutoff frequency. DGS ensures better in-band and out-of-band characteristics while achieving size reduction; this filter operates at (2.9-11.4) GHz, and the return loss S11 value exceeds -19.6dB. Our study of prior research on filter design revealed that the DGS approach was used in different geometric configurations and was mostly situated on the substrate bottom layer in most investigations.

The filter designer had to deal with a number of restrictions, such as restrained frequency ranges, limitations on size, limited design flexibility, and the difficulty of fabricating an exact dimensions model. Upon reviewing these researches, it was determined that most filters were large, the scattering parameter values required rise, and there was an absence of parametric optimization with conventional hairpin designs used. The identified issues can be addressed by decreasing the filter size concerning performance, enhancing the filter's response regarding scattering parameter values and bandwidth, substituting the dielectric material with a low-loss alternative, performing a parametric analysis of various parameters that impact the filter's efficiency, and altering the layout and placement of the DGS. This study aims to focus on the issue of narrow bandwidth in the passband region and moderate scattering parameter values. Its main goals are to increase the bandwidth and improve the scattering parameter values (S11, S21) while maintaining a small size and low cost for contemporary devices. Filter designers face difficulties in size reduction, such as increasing losses, a decrease in frequency range, sensitivity of manufacturing tolerances, and elevated costs. A balance between size reduction at minimal expense and optimal performance must be achieved. This research examines the design of a compact filter featuring distinctive hairpin-shaped resonators, enhancing the scattering parameter values through a parametric optimization of four critical parameters: resonator length (Lr), DGS area at the bottom layer, feed point position (t), and the spacing between two adjacent hairpin resonators (S1, S2). These four parameters are mainly selected because they directly impact the bandpass filter's performance. The resonator length will influence the bandwidth and resonant frequency, while the feed point location will determine impedance matching and affect the strength of the coupling. Additionally, resonators' distance from one another will impact their coupling, which is crucial for determining the filter's selectivity and bandwidth. This study presents a novel layout of a DGS added to the substrate's top and bottom layers, distinguishing it from prior research. The results indicate improved filter performance regarding in-band and out-of-band response, reduced overall size and enhanced scattering parameters. The substrate used is FR4, which has a substrate thickness of 1.6 mm and permittivity of 4.4 with a loss tangent of 0.02. The proposed filter was fabricated and evaluated to validate the results, yielding measurement outcomes closely aligned with the simulated data. Sections 2 and 3 arrange the remaining parts. Section 2 overviews the filter design steps, while Section 3 presents a parametric study. Section 4 then comprises the simulation outcomes and discussion. Section 5 includes the measurement results, followed by Section 6, which compares the suggested filter and previous work.

2. Proposed Filter Design

The proposed bandpass filter is constructed by using a five-hairpin resonator at the top layer. Each resonator is represented by a parallel inductor and capacitor, as illustrated in Figure 1, which displays the equivalent circuit schematic for five resonators, coupling capacitors between adjacent resonators represented by C12, C23, C34, and C45.

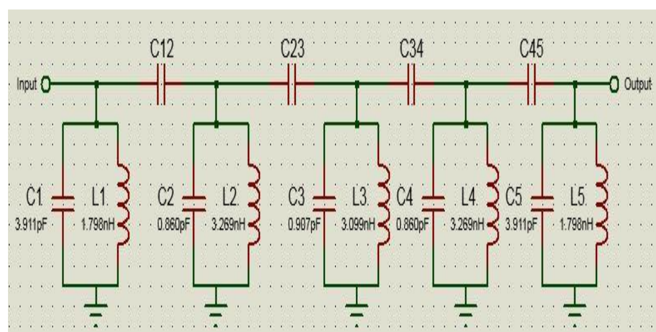

Fig. 1 Lumped elements of the hairpin resonators

A five-pole hairpin bandpass filter design intends to achieve a compromise between performance, sizes, and selectivity. The hairpin's shape was selected primarily on its compactness, ease of coupling, and optimum frequency response. Five hairpin resonators are often selected above three to increase resilience and capacity, which are crucial in high-performance systems. A hairpin resonator consists of a U-shaped configuration, a substrate, a ground plane, and a coupling section. These components collaborate to provide superior filter performance regarding selectivity, size, and bandwidth. Initially, the filter and substrate specifications should be determined, as shown in Table 1. Low pass values for the proposed filter (order five, ripple 0.1, and Chebyshev response) will be obtained from the standard Chebyshev table as follows: g0=1, g6=1, g1= 1.1468, g5 =1.1468, g2=1.3712, g4=1.3712, and g3=1.9750. The next steps must be followed:

Step (1) calculates the external quality factor at input and output ports denoted, respectively, by using the following Equations (1) and (2) [8].

$$Q_{e1} = \frac{g_0 g_1}{FBW}\ ,\ Q_{en} = \frac{g_n g_{n+1}}{FBW} \tag{1}$$

$$FBW = \frac{f_h - f_l}{f_o} \tag{2}$$

Where the fractional bandwidth of the filter is $\boldsymbol{FBW}$, $\boldsymbol{f_h}, \boldsymbol{f_l}$ represents the higher and lower cutoff frequencies at 2.1GHz and 3.8GHz, respectively, and $\boldsymbol{f_o}$ is the center frequency at 3GHz.

Step (2) The mutual coupling between resonators computed by using Equation (3),

$$M_{i,i+1} = \frac{FBW}{\sqrt{g_i g_{i+1}}} \tag{3}$$

Assumes that the spacing between two resonators is a specific value. Then, using the HFSS simulator, the filter is designed, and the S21 curve is examined. Take the two peaks of this curve and use Equation (4) to calculate the coupling coefficients k. The spacing between two adjacent hairpin resonators has different values, with S1 and S2 having 0.1mm and 0.2mm, respectively.

$$k = \frac{{f_h}^2 - {f_l}^2}{{f_h}^2 + {f_l}^2} \tag{4}$$

Step (3) the width of each resonator is calculated by Equations (5), and (6).

$$B = \frac{60\,\pi^2}{z_c\sqrt{\epsilon r}} \tag{5}$$

$$w/h = \frac{2}{\pi}\left\{\left((B-1)\right) - \ln(2B-1) + \frac{\epsilon r - 1}{2\epsilon r}\left[\ln(B-1) + 0.39 - \frac{0.61}{\epsilon r}\right]\right\} \tag{6}$$

Where h is the substrate thickness of 1.55mm and z_c represents characteristic impedance (50 ohms), the calculated width of each resonator is 1.5mm.

Step (4), the resonator length is equal to12mm, which is calculated by Equations (7)-(9).

$$k_0 = \frac{2\pi\, f_0}{c} \tag{7}$$

$$\epsilon_e = \frac{\epsilon r + 1}{2} + \frac{\epsilon r - 1}{2}\sqrt{\frac{1}{1 + 12(h/w)}} \tag{8}$$

$$L = \frac{\frac{\pi}{180^0}}{\sqrt{\epsilon_e}k_0} \tag{9}$$

Where $\boldsymbol{\epsilon_e}$ is an effective dielectric constant, and c denotes the speed of light in free space, while. Table 2 displays the dimensions of the upper layer and lower layer.

The selection of FR4 substrate is based on its cost-effectiveness and wide availability. The permittivity, thickness, loss tangent, and thermal stability of the FR4 substrate greatly impact how the hairpin resonator is designed, and these characteristics influence the filter's efficiency. A high dielectric constant enhances the compactness of the filter's size, but it also reduces its quality factor.

In order to improve filter response in terms of selectivity and size reduction, the DGS is introduced at the top layer as successive grooves for resonators 1 and 5, each measuring (0.5×1.5) mm^2. In addition, the DGS is used at the bottom layer of the proposed filter to enhance the scattering parameters, which are comprised of two narrow rectangular slots underneath the feed lines that have dimensions of (3×9) mm^2. The structures of both DGS are straightforward and easy to apply. Figures 2 and 3 depict the top layer and the final 3D representation of the suggested filter.

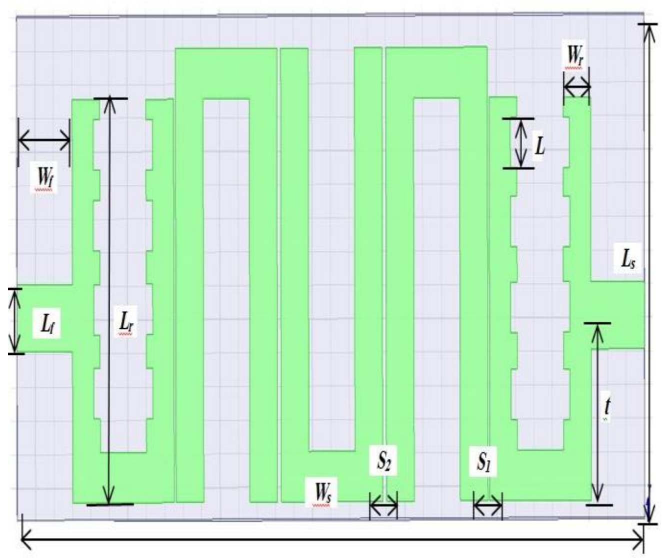

Fig. 2 The top layer of the proposed filter

Table 1. Specifications of proposed filter and substrate

Filter Parameter	Value
Lower cutoff frequency f_l	2.15GHz
Upper cutoff frequency f_h	3.85GHz
Center frequency f_0	3GHz
Order	5
Filter response	Chebyshev
Matching impedance	50 Ohm
Substrate type	FR4-epoxy
Substrate thickness h	1.55mm
Permittivity	4.4
Loss tangent	0.02

Table 2. Top and bottom layer dimensions

Filter Parameter	Value
Lower cutoff frequency f_l	2.15GHz
Upper cutoff frequency f_h	3.85GHz
Center frequency f_0	3GHz
Order	5
Filter response	Chebyshev
Matching impedance	50 Ohm
Substrate type	FR4-epoxy
Substrate thickness h	1.55mm
Permittivity	4.4
Loss tangent	0.02

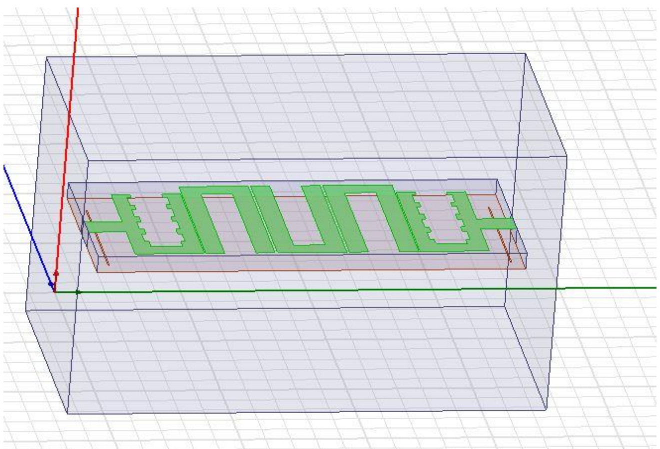

Fig. 3 3D view of the proposed filter

3. Parametric Study

The suggested filter has been designed and simulated using HFSS. This software package provides accurate simulation results, parametric optimization, scattering parameter extraction (S21 and S11), and quality factor computation. The simulation settings must be configured properly to achieve accurate and reliable results. These settings include assigning Perfect Electric Conductor (PEC) to all metallic parts at the top and bottom layers, exciting the structure using two lumped ports, assigning radiation boundary around the filter, defining the frequency range from 1GHz to 5GHz for 3GHz center frequency using fast sweep for quicker results. The filter's efficiency is determined by the insertion loss (S21) and return loss (S11) values. Signal attenuation is minimal in the passband area when insertion loss (S21) is near zero. A low return loss (S11 < -10) indicates effective impedance matching, resulting in less reflected signals and enhanced filter performance. This filter will experience a series of alterations in the feeding position, resonator length, space between resonators, and DGS area at the ground plane. The main objective is to get the scattering parameter values in an acceptable range. The optimization process of the four parameters was conducted manually by changing one parameter while keeping the others fixed. The feed point location *t* has been adjusted, and the small increase in feed point location changes the S11 and S21 values and the bandwidth. By adjusting the feeding position, superior impedance matching is attained, minimizing reflection and maximizing power transfer, which enhances filter efficiency, as seen in Figure 4. The optimal S11 is reached at *t* equal to 5.5mm, resulting in -56 dB, as illustrated in Table 3.

The filter response is affected by optimizing the space between two adjacent hairpin resonators (S1, S2). The simulation result when changing the values of *S1* and *S2* is illustrated in Figure 5. From the figure, the S21 and bandwidth will be affected significantly. The optimum results are obtained when the values of *S1* and *S2* equal 0.1mm and 0.2mm, respectively, as illustrated in Table 4. This behavior indicates that the proximity of the resonators enhances coupling, increasing the bandwidth and decreasing losses due to good signal transfers between the resonators.

Another parameter that can be optimized to investigate its effect on the filter performance is the length of two outer hairpin resonators, specifically (resonator 1 and resonator 5) *Lr*, as illustrated in Figure 6. The filter responses regarding bandwidth and S21 were slightly affected; however, the S11 value was greatly affected.

This behavior is due to the change in coupling strength, which subsequently affects the filter's bandwidth. Also, this change can affect return and insertion losses due to impedance mismatches or variations in resonance characteristics, as shown in Table 5.

Table 3. Simulated S-parameters with various values of *t*

Feed Point Position t (mm)	S21 (dB)	S11 (dB)	Bandwidth
5	-1.25	-41.8	2.25 - 3.85
5.5 (proposed)	-1.17	-56	2.15 - 3.88
6	-1.34	-42.27	2.31 - 3.73
6.5	-1.40	-42.38	2.23 - 3.76

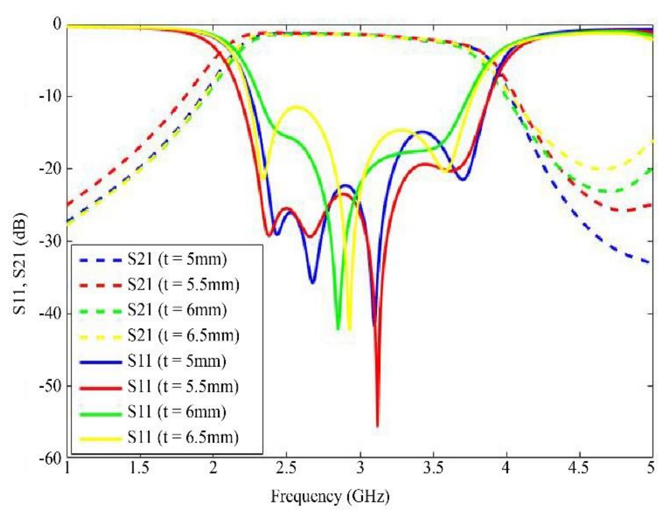

Fig. 4 Simulated S-parameter responses when varying feed point position t

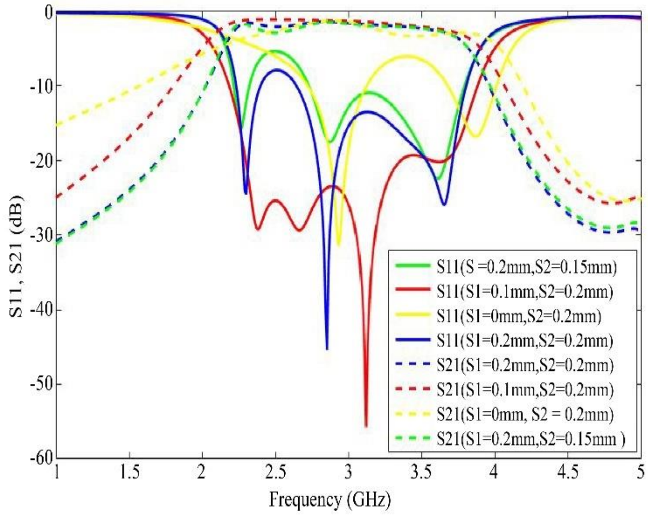

Fig. 5 Simulated S-parameter responses when varying S1 and S2 values

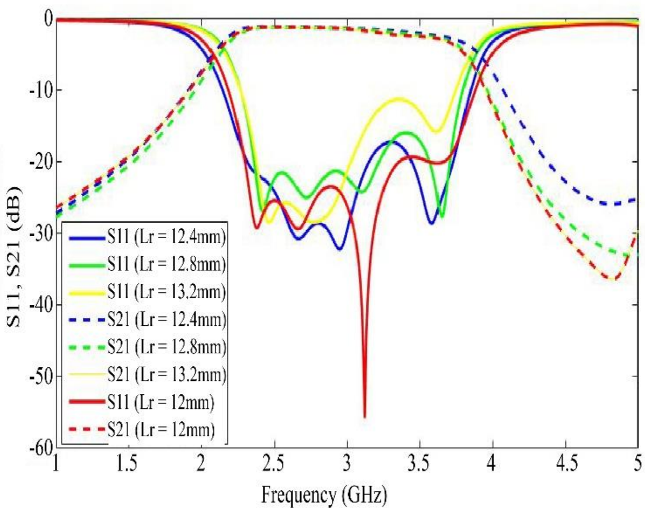

Fig. 6 Simulated S-parameter responses when varying Lr values

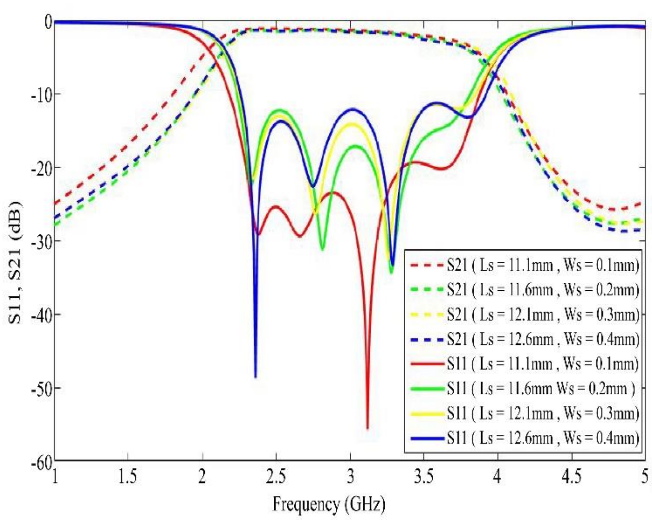

Fig. 7 Simulated S-parameter when changing the DGS Area

Table 4. Simulated S-parameters with various S1 and S2 values

Resonator length Lr (mm)	S21 (dB)	S11 (dB)	Bandwidth
12 (proposed)	-1.17	-56	2.15 - 3.88
12.4	-1.17	-32.21	2.14 - 3.84
12.8	-1.27	-27.75	2.25 - 3.78
13.2	-1.27	-28.46	2.26 - 3.74

Table 5. Simulated S-parameters with various values of Lr

Space between hairpin resonators S1 and S2 (mm)	S21 (dB)	S11 (dB)	Bandwidth
0.2 and 0.15	-1.5	-22.4	(2.20 - 2.30), (2.72 – 3.78)
0.1 and 0.2 (proposed)	-1.17	-56	2.15 - 3.88
0 and 0.2	-1.35	-31	(2.71-3.11), (3.67 – 4)
0.2 and 0.2	-1.5	-45.4	(2.22 – 2.39), (2.62 – 3.79)

Table 6. Simulated S-parameters with various areas of DGS

Area of DGS $(mm)^2$	S21 (dB)	S11 (dB)	Bandwidth
11.1×0.1 (proposed)	-1.17	-56	2.15 - 3.88
11.6×0.2	-1.37	-34.5	2.23 -3.81
12.1×0.3	-1.38	-32.5	2.23 - 3.84
12.6×0.4	-1.37	-48.7	2.25 - 3.91

The DGS at the ground plane is optimized, including a pair of thin, symmetric slots separated by a distance of 31.8mm. Figure 7 depicts the simulated scattering parameters. The figure shows that all of the S11 and S21 values and bandwidth are affected; the optimum results are obtained when the DGS area equals (11.1×0.1) $mm^{2,}$ where L_s and W_s represent the length and width of each slot. When reducing the area of DGS leads to reducing the capacitive and inductive effects and, as a result, enhances filter performance in terms of losses and bandwidth, as illustrated in Table 6.

4. Simulation Results and Discussion

HFSS software was first used to construct the suggested filter. The simulation results for several aspects of the filter design have been obtained and are described below:

4.1. Various Order Iterations

As part of an investigation into how the order of the filter affects its response, Figure 8 shows the simulated scattering parameters for several iterations of constructing the top layer of a hairpin bandpass filter. Where N denotes the number of resonators, in the first iteration (N=1), a single resonator is designed on the upper layer of the substrate; in the second iteration (N=3), three hairpin resonators are designed, while in the third iteration (N=5) a five-resonator is designed. From that figure, it is clear that when the filter order is increased to five, the return loss S11 value and selectivity will be improved significantly due to added resonators creating better impedance matching over the wide frequency range while degrading insertion loss S21 and increasing design complexity.

4.2. CST Simulation Results

The CST simulator validates the results previously acquired from the HFSS. Figure 9 compares two software simulators regarding their scattering parameters. This comparison can be used to evaluate the correctness of the simulated findings.

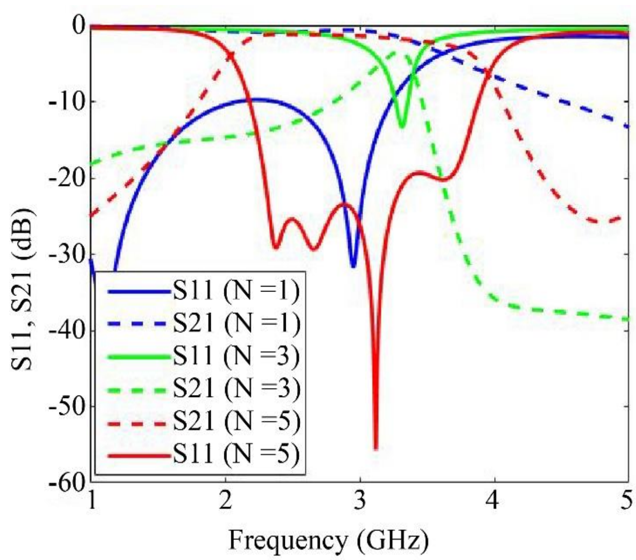

Fig. 8 Simulated S11 and S21 responses of various iterations for the filter order

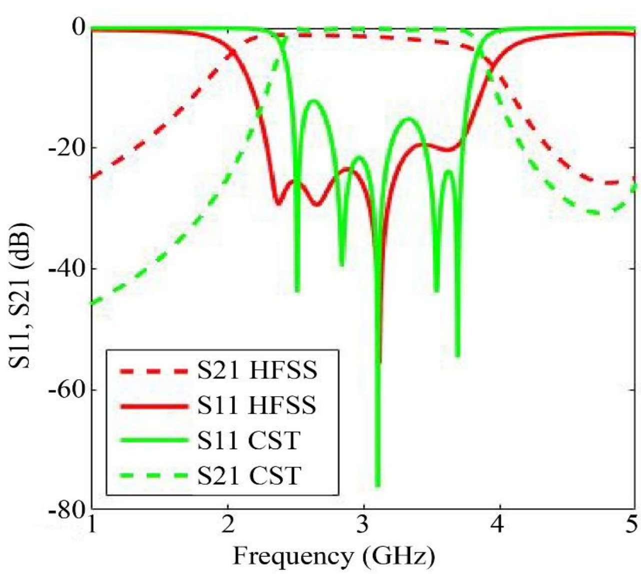

Fig. 9 Simulated S11 and S21 responses of the CST and HFSS simulators for the proposed filter

The figure indicates that the CST simulation results for scattering parameters exhibit a center frequency f_o at 3.1 GHz and lower and higher cutoff frequencies at 2.38GHz and 3.8 GHz, respectively. These results are close to those obtained from the HFSS simulator, especially near higher cutoff frequencies of 3.8GHz. The minor discrepancies between the two software are attributable to several factors, including the numerical approach, boundary conditions and excitations, meshing, and solver techniques.

4.3. Group Delay Current Distribution

Group delay, a crucial factor in maintaining the signal's shape and preventing distortion, is another parameter for evaluating the filter performance. In this design, the group delay is flat at the passband region from 2.15GHz to 3.88GHz, as illustrated in Figure 10. The more stable the group delay in the passband region, the better. Eventually, the surface current distribution of the presented filter at the center frequency of 3GHz is depicted in Figure 11, which indicates a current flow appears at five hairpin resonators.

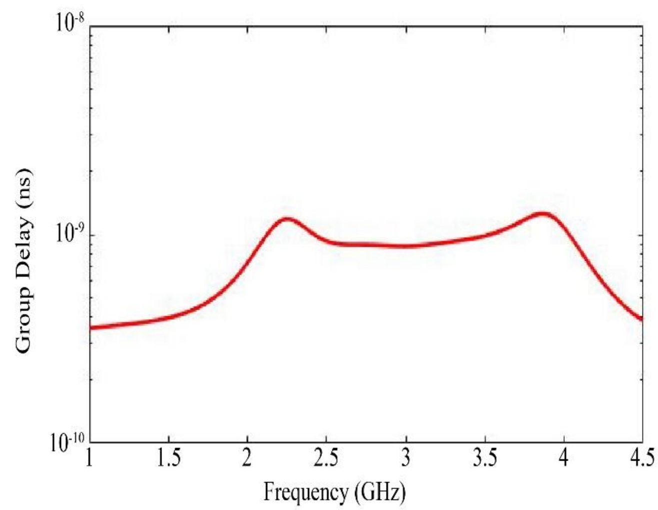

Fig. 10 Group delay of the presented filter

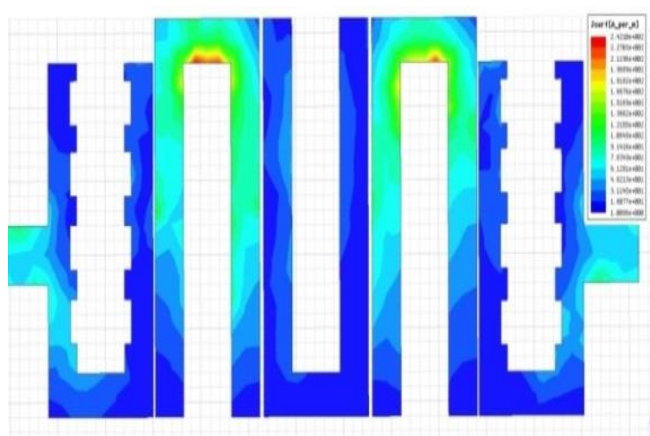

Fig. 11 The distribution of surface currents in the presented filter at 3GHz

5. Experimental Results

The presented filter was manufactured on an FR4 substrate and tested for real-time validation. The primary objective of verifying the design with the fabricated prototype and CST is to guarantee that the theoretical performance of the filter is consistent with real-world behaviors. This dual verification process is crucial for determining any discrepancies, design optimization, and impacts of the manufacturing process, as well as for the assurance that the final product complies with industry standards and design specifications. The measurement results are obtained by using the Vector Network Analyzer (VNA) MS4642A, which is connected to the fabricated model through two SMA connectors, as exhibited in Figure 12. Figure 13 illustrates the distinction between the simulated and realized scattering parameter findings. The measured return and insertion losses for the bandpass region are -30 dB and -1.18 dB. The measured bandwidth of the filter is (2.8 -3.75) GHz. The figure indicates that the measurement outcomes align well with the simulation outcomes. The differences may occur due to mismatches of SMA connectors, losses of the FR4 substrate, fabrication tolerance, and external measurement conditions. Electromagnetic interference and temperature are the two main environmental factors that affect the fabrication results.

The main challenge encountered during the manufacturing process of this filter is pattern accuracy, which is managed by using etchings with dimensions that are suitable for the cutting machine and utilizing simple structures of DGS to avoid the complexity of the design. The suggested filter is suitable for several recent wireless communication systems that need filters with sharp cutoffs and high selectivity to distinguish the desired signal band from interference and noise. The suggested filter may be used for 5G applications like the Internet of Things (IoT), autonomous vehicles, and improved mobile broadband. As well as it can be used for radar and satellite communications.

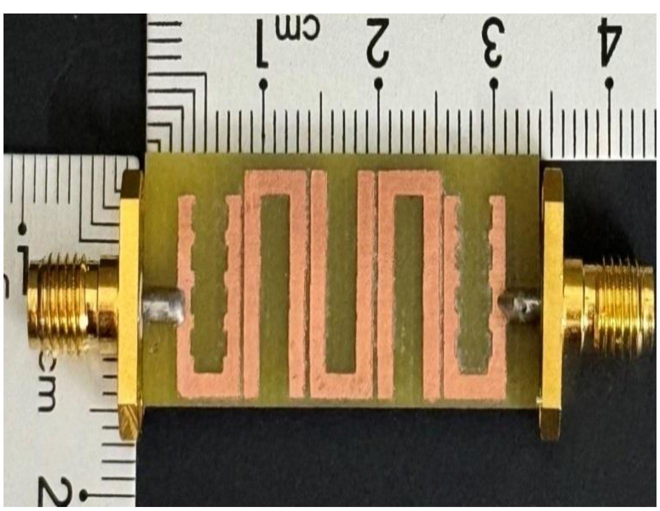

(a) Upper view

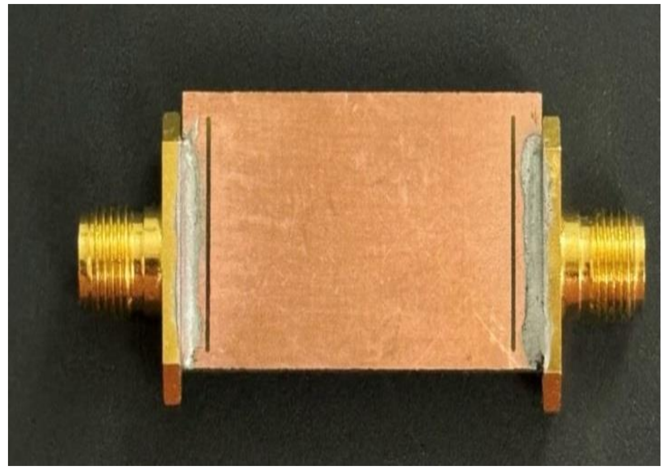

(b) Lower view

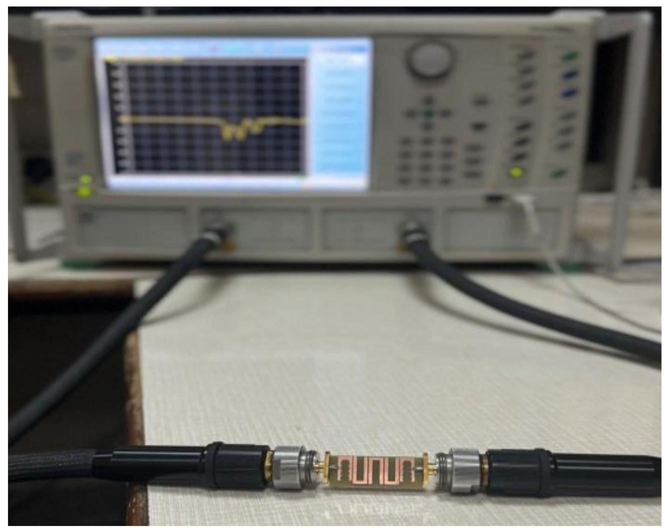

(c) VNA

Fig. 12 Photograph of the prototype filter (a) Upper view, (b) Lower view, and (c) VNA (MS4642A).

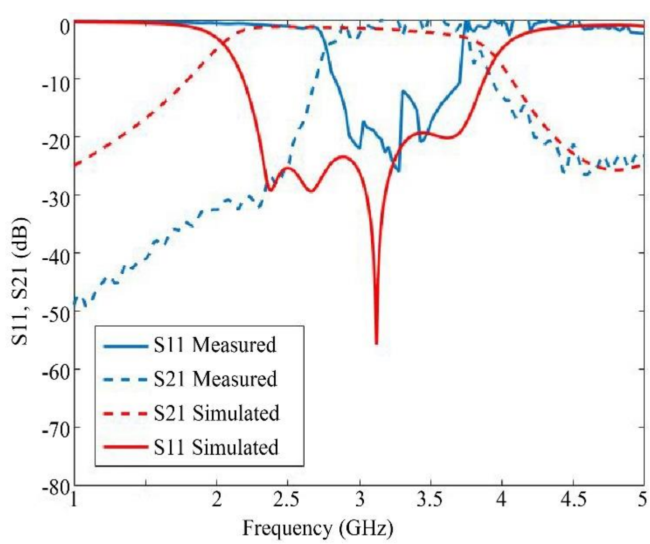

Fig. 13 Simulation and measurement scattering parameters' findings

Table 7. Proposed filter comparison with other existing references

Ref No.	S21 (dB)	S11 (dB)	BW (MHz)	Center Frequency (GHz)	Filter Size $(mm)^2$
[19]	-0.2946	-46.64	460	2.22	18.2×34.8
[21]	-0.76	-29	200	3	53.7×17.6
[22]	-0.1	-24	600	2.2	49×25
[23]	-3	-41	250	2.35	70×45
This Work	-1.17	-56	1700	3	15×34

6. Comparison with Other References

The proposed filter is compared with previous studies [19-23] at different frequency ranges, focusing on scattering parameters, center frequency, bandwidth, and size highlighted in Table 7. As the table shows, this filter has a simple structure; it provides the best S21, S11, and wider bandwidth, equal to -1.17dB, -56dB, and (2.15 - 3.88) GHz, respectively. Also, it has the smallest size compared to others, which is equal to (15×34) mm^2.

7. Conclusion

This research analyses simulates, and fabricates a new bandpass filter design with DGS. 5G applications, radar, and satellite communications can use the suggested filter. This study employs two distinct DGS at the upper and lower layers to improve the scattering parameters, compactness, and bandwidth widening. This filter was initially designed by HFSS software, focusing on a parametric study to find the optimal filter response by varying the feeding position, resonator length, space between resonators, and DGS area at the ground plane.

The optimized values of four significant parameters are the 12mm resonator length Lr, the (11.1×0.1) mm^2 area of DGS, the 5.5mm feed point position *t*, and the 0.1mm and 0.2mm spacing between two adjacent hairpin resonators. The CST simulator is used to verify the results previously obtained by HFSS. The fabricated results indicated slight differences from the simulated ones due to SMA connector mismatch, manufacturing tolerance, and losses in the FR4 substrate. This filter offers a wider bandwidth of (2.15 - 3.88) GHz at the 3 GHz center frequency, excellent return loss and insertion loss of -56.19dB and -1.17dB, respectively, flat group delay, and a simple design. Future work can apply distinct methods to the proposed filter for further improvements, including changing the substrate material type, more miniaturization, and conducting parametric optimization with another parameter.

References

[1] Qazwan Abdullah et al., “A Compact Size 5G Hairpin Bandpass Filter with Multilayer Coupled Line,” *arXiv*, pp. 1-15, 2021. [CrossRef] [Google Scholar] [Publisher Link]

[2] Sonu Jain et al., “Novel Hairpin Band-Pass Filter Using Tuning Stub,” *Proceedings of International Conference on Data Science and Applications*, pp. 145-152, 2020. [CrossRef] [Google Scholar] [Publisher Link]

[3] Eman Gamal Ouf et al., “Electronically Switchable Ultra-Wide Band/Dual-Band Bandpass Filter Using Defected Ground Structures,” *Progress in Electromagnetics Research C*, vol. 91, pp. 83-96, 2019. [CrossRef] [Google Scholar] [Publisher Link]

[4] M.M. Ma et al., “Tri-Band Cross-Coupling Bandpass Filter with Rectangular Defected Ground Structure Array,” *Journal of Electromagnetic Waves and Applications*, vol. 32, no. 11, pp. 1409-1415, 2018. [CrossRef] [Google Scholar] [Publisher Link]

[5] Lung-Hwa Hsieh, and Kai Chang, “Compact, Low Insertion-Loss, Sharp-Rejection, and Wide-Band Microstrip Bandpass Filters,” *IEEE Transactions on Microwave Theory and Techniques*, vol. 51, no. 4, pp. 1241-1246, 2003. [CrossRef] [Google Scholar] [Publisher Link]

[6] Elmahjouby Sghir et al., “Miniaturized Ultra-Wideband Coplanar Wave Guide Lowpass Filter with Extended Stop Band,” *Indonesian Journal of Electrical Engineering and Computer Science*, vol. 19, no. 3, pp. 1415-1419, 2020. [CrossRef] [Google Scholar] [Publisher Link]

[7] Sergio Mora et al., “Design of a Bandpass Filter Using Microstrip Hairpin Resonators,” *2017 CHILEAN Conference on Electrical, Electronics Engineering, Information and Communication Technologies*, Pucon, Chile, pp. 1-5, 2017. [CrossRef] [Google Scholar] [Publisher Link]

[8] Norfishah Abd Wahab et al., “Design a Microstrip Hairpin Band-Pass Filter for 5GHZ Unlicensed WiMAX,” *2010 International Conference on Networking and Information Technology*, Manila, Philippines, pp. 183-186, 2010. [CrossRef] [Google Scholar] [Publisher Link]

[9] Giovanni Gugliandolo et al., “On the Development of Inkjet-Printed Band Pass Filters Based on the Microstrip Hairpin Structure,” *Instruments*, vol. 8, no. 1, pp. 1-15, 2024. [CrossRef] [Google Scholar] [Publisher Link]

[10] David M. Pozar, *Microwave Engineering*, Wiley, pp. 1-732, 2012. [Google Scholar] [Publisher Link]

[11] A.B. Abdel-Rahman et al., “Control of Bandstop Response of Hi-Lo Microstrip Low-Pass Filter Using Slot in Ground Plane,” *IEEE Transactions on Microwave Theory and Techniques*, vol. 52, no. 3, pp. 1008-1013, 2004. [CrossRef] [Google Scholar] [Publisher Link]

[12] N. Chami, D. Saigaa, and A. Djaiz, “A New Miniature Micro-Strip Two-Layer Band-Pass Filter Using Aperture-Coupled Hairpin Resonators,” *Engineering, Technology & Applied Science Research*, vol. 12, no. 4, pp. 9038-9041, 2022. [CrossRef] [Google Scholar] [Publisher Link]

[13] Sheng Sun, and Lei Zhu, “Wideband Microstrip Ring Resonator Bandpass Filters under Multiple Resonances,” *IEEE Transactions on Microwave Theory and Techniques*, vol. 55, no. 10, pp. 2176-2182, 2007. [CrossRef] [Google Scholar] [Publisher Link]

[14] A. Djaiz, and A. Denidni, "A New Compact Microstrip Two-Layer Bandpass Filter Using Aperture-Coupled SIR-Hairpin Resonators with Transmission Zeros," *IEEE Transactions on Microwave Theory and Techniques*, vol. 54, no. 5, pp. 1929-1936, 2006. [CrossRef] [Google Scholar] [Publisher Link]

[15] Amel Ramdedović, and Sehabeddin Taha Imeci, "Tight-Coupled Microstrip Hairpin Bandpass Filter," *Journal of Engineering Research*, vol. 11, no. 1A, pp. 212-222, 2023. [Google Scholar] [Publisher Link]

[16] K. Kavitha, and M. Jayakumar, "Design and Performance Analysis of Hairpin Bandpass Filter for Satellite Applications," *Procedia Computer Science*, vol. 143, pp. 886-891, 2018. [CrossRef] [Google Scholar] [Publisher Link]

[17] Sio-Weng Ting, Kam-Weng Tam, and R.P. Martins, "Miniaturized Microstrip Lowpass Filter with Wide Stopband Using Double Equilateral U-Shaped Defected Ground Structure," *IEEE Microwave and Wireless Components Letters*, vol. 16, no. 5, pp. 240-242, 2006. [CrossRef] [Google Scholar] [Publisher Link]

[18] A. Boutejdar, A. Elsherbini, and A. Omar, "Design of Novel Hairpin-DGS Microstrip Bandpass and Lowpass Filters Using Coupling Matrix Method," *German Microwave Conference*, Hamburg, Germany, pp. 261-265, 2008. [Google Scholar] [Publisher Link]

[19] Vivek Singh Kushwah, Sarita Singh Bhadauria, and Geetam Singh Tomar, "Design of Microstrip Hairpin-Line Bandpass Filter with Square Shape Defected Ground Structure," *Asia-Pacific Journal of Advanced Research in Electrical and Electronics Engineering*, vol. 1, no. 1, pp. 21-38, 2017. [CrossRef] [Google Scholar] [Publisher Link]

[20] Jagadish Baburao Jadhav, and Pramod Jagan Deore, "A Compact Planar Ultra-Wideband Bandpass Filter with Multiple Resonant and Defected Ground Structure," *AEU - International Journal of Electronics and Communications*, vol. 81, pp. 31-36, 2017. [CrossRef] [Google Scholar] [Publisher Link]

[21] Nanang Ismail et al., "Design of Microstrip Hairpin Bandpass Filter for 2.9 GHz–3.1 GHz s-Band Radar with Defected Ground Structure," *Malaysian Journal of Fundamental and Applied Sciences*, vol. 14, no. 4, pp. 448-455, 2018. [CrossRef] [Google Scholar] [Publisher Link]

[22] Hassan Sajjad et al., "A Compact Hairpin Filter with Stepped Hairpin Defected Ground Structure," *2018 IEEE 21st International Multi-Topic Conference (INMIC)*, Karachi, Pakistan, pp. 1-5, 2018. [CrossRef] [Google Scholar] [Publisher Link]

[23] M. Nedelchev, and A. Kolev, "Synthesis of Planar Filters Using Defected Ground Structure Miniaturized Hairpin Resonators," *Engineering, Technology & Applied Science Research*, vol. 9, no. 1, pp. 3734-3738, 2019. [CrossRef] [Google Scholar] [Publisher Link]

[24] N. Ambati et al., "Parametric Analysis of the Defected Ground Structure-Based Hairpin Band Pass Filter for VSAT System on Chip Applications," *Engineering, Technology & Applied Science Research*, vol. 11, no. 6, pp. 7892-7896, 2021. [CrossRef] [Google Scholar] [Publisher Link]

[25] Ravi Prakash Verma, Bhagirath Sahu, and Ashish Gupta, "A Miniaturized UWB Bandpass Filter with Tunable Cut-Off Frequencies Employing Rectangular Open-Loop Defected Ground Structure," *International Journal of Microwave and Wireless Technologies*, vol. 15, no. 10, pp. 1689-1697, 2023. [CrossRef] [Google Scholar] [Publisher Link]